Model of Reactor for Plasma Treatment of Dispersed Water-organic Nitrate Solutions of Metals

Alexander Karengin[a)], Alexey Karengin, Ivan Novoselov and Nikita Golovkov

Tomsk Polytechnic University, 30 Lenina Avenue, Tomsk 634050 Russian Federation

[a)]Corresponding author: karengin@tpu.ru

Abstract. The paper proposes a mathematical model of the reactor, which describes the process of treatment of dispersed water-organic nitrate solutions of metals at air-plasma flow temperatures more than 1500 K. Regularities and a quantitative comparison were made to show the effect of the initial values of the air-plasma flow parameters (temperature, velocity) and the WONS droplet parameters (size, velocity) on the rate of their evaporation in the reactor. Process conditions were established that ensure a high evaporation rate of dispersed solutions in the air-plasma flow.

INTRODUCTION

One of the promising areas for further development of nuclear energy is the creation of fuel compositions (FC), including fissionable metal oxides (uranium, plutonium, and thorium) and a matrix of metal oxides (beryllium, magnesium, etc.) with high thermal conductivity and low cross section for resonant neutron absorption [1-5].

Promising technique to obtain FC is the use of air plasma. However, obtaining FC in air plasma from dispersed mixed water nitrate solutions of metals requires significant energy consumption (till 4.0 kWh/kg) and additional hydrogen reduction to obtain compositions of the required phase composition [5–9].

The advantages of obtaining FC in air plasma from dispersed mixed water nitrate solutions of metals, including the organic component, include low energy consumption (till 0.1 kW h/kg) and obtaining compositions of the required phase composition without additional hydrogen reduction [10-12].

The diversity and complexity of the processes occurring in the reactor during plasma processing of dispersed solutions, their lack of knowledge, and the lack of reliable experimental methods for diagnosing high-temperature two-phase flows with phase transitions require the use of mathematical modeling methods.

The authors of [13] developed a model describing the evaporation process of droplets of water treatment waste from water suspensions of metal hydroxides in an air-plasma stream in the form of water-organic compositions.

In this paper, we propose a mathematical model of the reactor, which describes the process of plasma processing of dispersed water-organic nitrate solutions (WONS), including mixed water-nitrate solutions of fissile metals (uranium, plutonium, thorium), matrix metals (beryllium, magnesium, etc.) and the organic component (alcohols, ketones).

The purpose of this work is to establish regularities and quantitative comparison of the effect of the initial values of the parameters of the air-plasma flow (temperature, speed) and WONS droplets (size, speed), their initial mass ratio on the kinetics of the process and the definition of modes that provide high speed plasma processing of dispersed WONS.

CALCULATION OF BURNING INDEXES AND COMPOSITIONS OF WONS

Lower heat value and adiabatic combustion temperature of WONS including organic component (ethanol, acetone) and mixed water-nitric solutions of fissile materials (uranium, plutonium, and thorium) and matrix materials (beryllium and magnesium) are determined from formulas (1) and (2) [13]:

V International Conference for Young Scientists, Post-Graduate Students and Students
AIP Conf. Proc. 2101, 020016-1–020016-6; https://doi.org/10.1063/1.5099608
Published by AIP Publishing. 978-0-7354-1831-8/$30.00

$$Q_l = \frac{(100 - W - A) \cdot Q_{lc}}{100} - \frac{2.5 \cdot W}{100}, \quad (1)$$

where Q_{lc} is lower heat value of combustible component of WONS, MJ/kg; W and A are content of water and noncombustible components in WONS, wt.%.

$$T_{ad} = \frac{Q_l + C_{WONS} \cdot t_{WONS} + \alpha \cdot \upsilon_{OX} \cdot C_{OX} \cdot t_{OX}}{V \cdot C}, \quad (2)$$

where C_{WONS} – average mass heat capacity of WONS [kJ/kg], t_{WONS} – temperature of WONS [°C], α – oxidant flow coefficient, υ_{OX}– theoretical flow of oxidant [m^3/m^3], C_{OX} – average heat capacity of oxidizer [kJ/(m^3·°C)], t_{OX} – temperature of oxidizer [°C], V – specific volume of WONS plasma treatment products [m^3/kg], C – specific equilibrium heat capacity of WONS plasma treatment products [kJ/(m^3·°C)].

As a result of the calculations, the optimal composition of WONS was determined. These compositions have $Q_l \geq 8.4$ MJ/kg, $T_{ad} \geq 1500$ K, and provides plasma energy-efficient production of complex oxide compounds for dispersion nuclear fuel of various chemical compositions [12]: UO_2–MgO, UO_2–BeO, PuO_2–UO_2–MgO, PuO_2–UO_2–BeO, etc.

MODEL OF REACTOR FOR PLASMA TREATMENT OF DISPERSED WATER-ORGANIC NITRATE SOLUTIONS OF METALS

Air-plasma flow, carrying droplets of WONS in reactor can be figuratively divided into several zones (Fig. 1). Mixing of flow and heating up of droplets to evaporation temperature occurs in zone (0-1), droplets undergo dynamic evaporation in zone (1-2), salt residue is formed and heated up to decomposition temperature in zone (2-3), salt residue is dissolved into gaseous and solid components in zone (3-4).

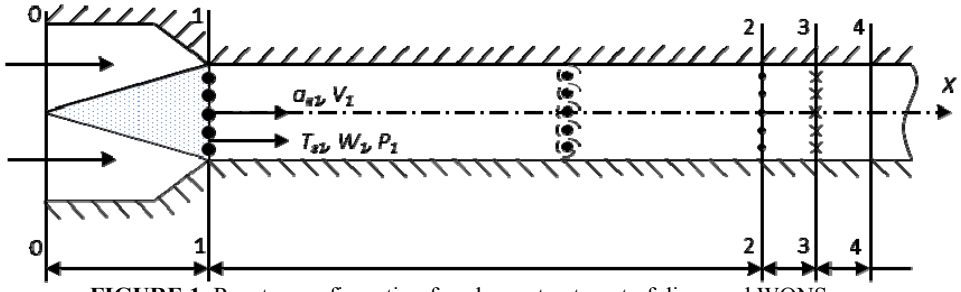

FIGURE 1. Reactor configuration for plasma treatment of dispersed WONS.

Conducted comparative assessment show that by temperature 1500 K and higher, as a limiting process can be considered stage (1-2) of solvent evaporation [13].

When developing the reactor model, the following assumptions were taken: plasma reactor is a reactor of ideal displacement; the considered processes are quasi-stationary; air-plasma flow is adiabatic; droplets are monodispersed, not interacting with each other and reactor walls; chemical reactions between air-plasma heat carrier and moisture vapor do not occur.

To describe one-dimensional two-phase flow with phase transitions along the length of reactor evaporation zone were used equations (3–10) [13]:

- equation describing droplet evaporation in conditions when evaporation velocity is defined by heat input:

$$\frac{dm_d}{d\tau} = -\pi Nu^* \frac{\lambda_s (T_g - T_p)}{\Delta H^*} \alpha_d, \quad (3)$$

where

$$Nu^* = 2\phi(\mathrm{Re})\psi_R H_1(B); \; H_1(B) = \frac{\ln(1+B)}{B}; \; \phi(\mathrm{Re}) = 1 + 0{,}3\,\mathrm{Re}^{\frac{1}{2}}\,\mathrm{Pr}^{\frac{1}{3}}; \; B = \frac{c_{ps}(T_g - T_p)}{\Delta H^*}$$

$$\psi_R = 1 + r_0(\phi(\mathrm{Re})H_1(B))^{-1}; \; \mathrm{Re} = \alpha_d \rho_g |W - V| \eta_g^{-1}; \; P_r = C_{pg}\eta_g / \lambda_g;$$

- equation of droplet motion:

$$m_d \frac{dV}{d\tau} = \frac{\pi}{8} C_d^{\,*} \rho_g \alpha_d^{\,2} |W - V| (W - V), \quad (4)$$

where

$$C_d^{\,*} = C_d(\mathrm{Re})H_2(\mathrm{Re}, B)\psi(We), \; B^* = \ln(1+B)/\mathrm{Pr};$$

$$C_d(\mathrm{Re}) = 0,32 + 4,4\,\mathrm{Re}^{-0,5} + 24\,\mathrm{Re}^{-1},\ \mathrm{Pr} = \eta_s c_{ps} \lambda_s^{-1};$$

$$\phi(We) = \exp(0.003We^{3/2}),\ \ We = \alpha_d \rho_g (W-V)^2 \sigma_q^{-1};$$

$$H_2(\mathrm{Re}, B) = 1 - \left[0,25B^* / (1 + 0,01\mathrm{Re} + 0,2B^*\,\mathrm{Re}^{-1}\right];$$

- droplet velocity:

$$\frac{dx}{d\tau} = V; \tag{5}$$

- droplet evaporation law:

$$z_v = 1 - \left(\frac{\alpha_d}{\alpha_{d1}}\right)^3 \frac{\rho_q}{\rho_{q1}}; \tag{6}$$

- conservation law of two-phase mixture:

$$\frac{d}{d\tau}(W\rho F + m_q) = 0; \tag{7}$$

- conservation law of mixture impulse:

$$\frac{d}{d\tau}(mW + m_q B + PF) = P\frac{dF}{d\tau}, \tag{8}$$

where $m = m_g + m_p$;

- energy conservation law of two-phase mixture

$$\frac{d}{d\tau}\left[m\left(I_s + \frac{W^2}{2}\right) + m_q\left(I_q + \frac{V^2}{2}\right) + m_s \Delta H^*\right] = 0; \tag{9}$$

- constitutive equation of vapor-gas mixture

$$\frac{P}{\rho} = \frac{RT}{\mu(T)}, \tag{10}$$

where $1/\mu(T) = r_g/\mu_g(T) + r_v/\mu_v(T)$.

In equations (3-10): r_g and r_v – mass ratio of air and water vapor; τ - time; W and V – velocities of air-plasma flow and droplets; T_{g1} – initial temperature of air flow; P – pressure; ρ – density; F – cross section area of reactor; H – enthalpy; μ – molecular weight; λ – thermal conductivity coefficient; η – dynamic viscosity coefficient; C_p and C_v – heat capacity at constant pressure and volume; α_d – droplet size; m – mass. For these parameters the following indices were used: q– liquid, g – gas, v – vapor, d – droplet; s – mixture of gas and vapor, figure 1 for initial parameters.

Thermal and physical values of air-plasma flow and water vapor necessary for calculations were taken from [14,15] depending on the temperature and were approximated by algebraic polynomials. Values η_s, λ_s, C_{ps} were roughly defined from the equation (11) by average temperature value T_{av} and vapor concentration C:

$$T_{av} = \frac{T_g + T_{eq}}{2},\ C = \frac{C_0 + C_\infty}{2}, \tag{11}$$

where C_0 and C_∞ – vapor concentration at droplet surface and in approaching flow, T_{eq} – droplet equilibrium evaporation temperature. When $T_g > T_{eq}$ we can accept that $T_{eq} = T_b$ (boiling temperature), $C_0 = 1$ and therefore $C_\infty = \beta z_v(1 + \beta z_v)$. Thermal conductivity and viscosity of steam and gas mixture were defined using Vasiliev and Wilk formulas [15].

CALCULATION RESULTS OF EVAPORATION KINETICS FOR DROPLETS OF DISPERSED WONS AND THEIR DISCUSSION

The obtained system of differential equations (3-10), after their transformation to linearity was solved using Runge-Kutta method [13]. Accuracy when defining normalized parameters did not exceed 0.1 %.

The calculations were held for the following initial parameters: droplet diameter α_{d1} = (40÷100) μm; droplet velocity V_1 = (10÷100) m/s; flow velocity W_1 = (10÷90) m/s; flow temperature T_{g1} = (2000÷4000) K; initial mass ratio of WONS droplets and air-plasma flow β = (0.1÷1.5); pressure P_1 = 0.1 MPa.

Figures 2-6 illustrate the calculation results. Figure 2 shows influence of initial mass ratio of liquid and gaseous phases β (at a_{d1}=100 μm, V_1=100 m/s, W_1=30 m/s) on final temperature of air-plasma flow at the end of reactor evaporation zone (a) and length x_{evap}, where droplets evaporate completely (b).

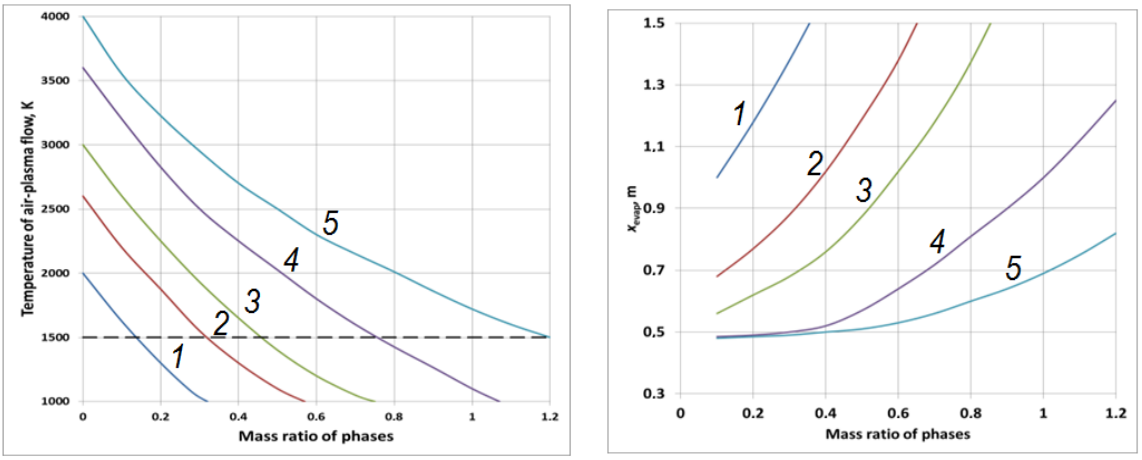

(a) (b)

FIGURE 2. Influence of initial mass ratio of phases on end temperature of air-plasma flow (a) and length of zone of complete droplet evaporation (b) in reactor: 1 – T_{g1} = 2000 K; 2 – 2600 K; 3 – 3000 K; 4 – 3600 K; 5 – 4000 K.

The dependency analysis shows (Fig. 2a) that β strongly influences on the final temperature of air-plasma flow T_{end}. Exceeding $\beta > \beta^*$ (Fig. 2b) leads to sharp decrease of flow temperature at the initial stage and significant increase of x_{evap}. Obtained dependences allow for a given initial temperature of the stream T_{g1} to select such $\beta = \beta^*$ (dashed line), which provides at the end of the zone of complete evaporation of the droplets the final temperature of the stream $T_{end} \approx 1500$ K. For T_{g1} = 2000 K, 2600 K, 3000 K, 3600 K, and 4000 K β equals 0.14, 0.26, 0.45, 0.76, and 1.20.

Figure 3 shows the influence of initial temperature of air-plasma flow T_{g1} on $\boldsymbol{x}_{evap}$ (at $\beta = \beta^*$) for the initial flow velocity of 10 and 90 m/s and the initial mass weight of phases β^*, providing $T_{end} \approx 1500$ K at the end of complete evaporation zone.

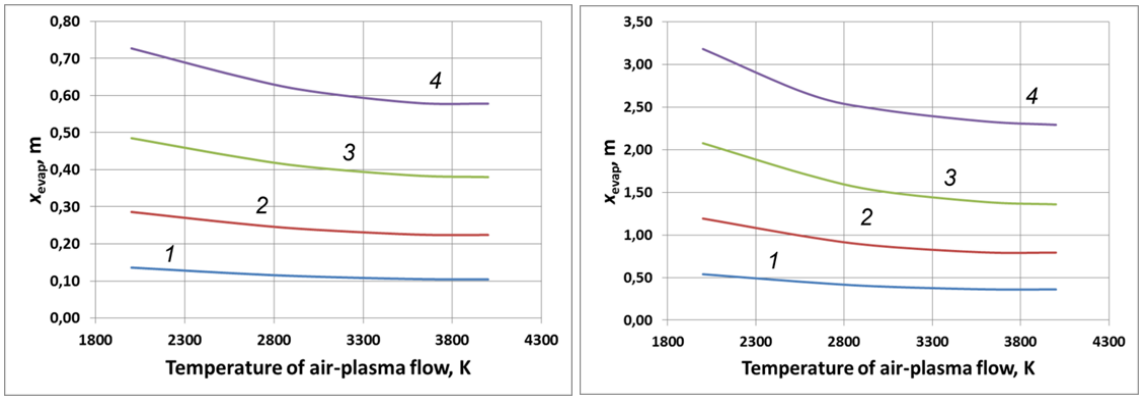

(a) (b)

FIGURE 3. Influence of initial temperature of air-plasma flow T_{g1} (at $\beta = \beta^*$) on the length of droplet full evaporation zone $\boldsymbol{x}_{evap}$ for the initial flow velocity 10 m/s (a) and 90 m/s (b): 1 – a_{d1}= 40 µm; 2 – 60 µm; 3 – 80 µm; 4 – 100 µm.

Analyzing the obtained dependencies shows that T_{g1} (at $\beta=\beta^*$) does not influence x_{evap} significantly and increase of initial temperature of air-plasma flow from 2000 K to 3600 K leads to gradual decrease of x_{evap}. Significant influence (at $\beta=\beta^*$) of initial droplet size on x_{evap} should be noted. Thus, reduction of initial droplet size from 100 µm to 40 µm leads to sharp decrease of x_{evap} (by 5-6 times), while increase of initial velocity of air-plasma flow W_1 from 10 m/s to 90 m/s leads to sharp increase of x_{evap} (by 4-5 times).

Figure 4 illustrates the influence of initial velocity of air-plasma flow W_1 on $\boldsymbol{x}_{evap}$ for the initial flow temperature of 2000 and 4000 K at $\beta=\beta^*$, providing $T_{end} \approx 1500$ K at the end of complete evaporation zone.

Analysis of the obtained graphs (Fig. 4a, Fig. 4b) indicates that increase of W_1 from 10 m/s to 90 m/s leads to sharp increase in x_{evap} (by 4-5 times), while reduction of a_{d1} from 100 µm to 40 µm – to sharp decrease of x_{evap} (by 5-6 times). Increase of T_{g1} flow from 2000 K (a) to 4000 K (b) (at $\beta=\beta^*$) does not have significant influence on x_{evap}.

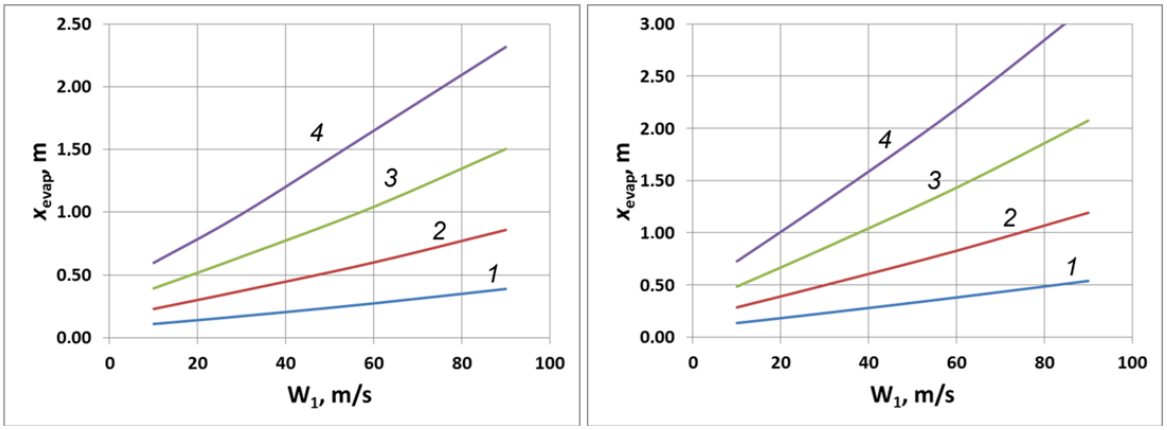

(a) (b)

FIGURE 4. Influence of initial velocity of air-plasma flow W_1 on the length of droplet complete evaporation zone $\boldsymbol{x}_{evap}$ for the initial flow temperature 2000 K (a) and 4000 K (b): 1 – a_{d1}= 40 μm; 2 – 60 μm; 3 – 80 μm; 4 – 100 μm.

The influence of a_{d1} on x_{evap} for the initial temperature of air-plasma flow of 2000 and 4000 K (at β=β*), providing T_{end}≈ 1500 K at the end of the zone of complete droplet evaporation is given in Fig. 5.

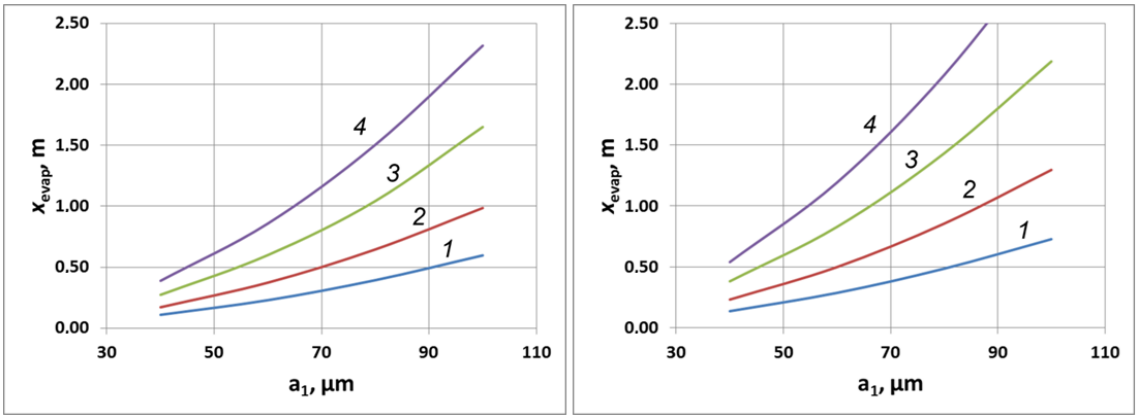

(a) (b)

FIGURE 5. Influence of initial droplet size a_{d1} on the length of droplet complete evaporation zone in reactor for the initial temperature of air-plasma flow 2000 K (a) and 4000 K (b): 1 – W_1= 10 m/s; 2 – 30 m/s; 3 – 60 m/s; 4 – 90 m/s.

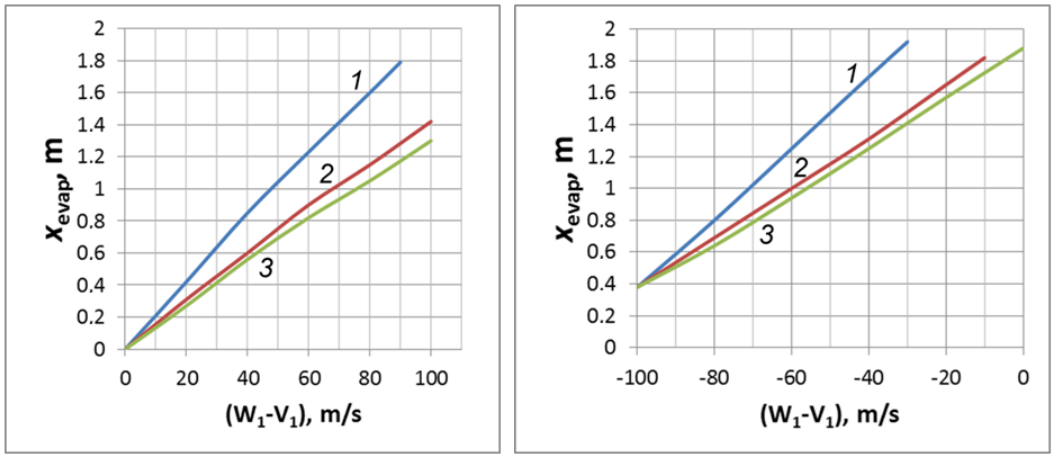

(a) (b)

FIGURE 6. Influence of initial velocity of droplets blow by air-plasma flow on the length of droplet complete evaporation in reactor at the initial droplet size α_{d1}=100 μm and initial droplet velocity V_1 0 m/s (a) and 100 m/s (b): 1 – T_{g1}=2000 K; 2 – 3000 K; 3 – 4000 K.

Analysis of the obtained dependencies (Fig. 5a and 5b) makes possible to state that reduction of initial droplet size from 100 μm to 40 μm leads to sharp decrease of x_{evap} (by 5-6 times), and reduction of W_1 from 90 m/s to 10 m/s leads to sharp decrease of x_{evap} (by 4-5 times). Along with that, increase of T_{g1} from 2000 K (5a) to 4000 K (5b) (when $\beta = \beta^*$) does not influence x_{evap} significantly.

Figure 6 demonstrates the influence of initial velocity of droplet blow (W_1-V_1) by air-plasma flow on x_{evap} at the initial droplet size α_{d1}=100 μm and initial droplet velocity 0 and 100 m/s (at $\beta=\beta^*$), providing $T_{end} \approx$ 1500 K at the end of droplet complete evaporation zone.

Analyzing the obtained data it can be concluded that increase of droplet blow velocity from 0 to 100 m/s does not lead to significant decrease of x_{evap} and is mainly defined by the initial velocity of air-plasma flow W_1. It should also be noted that reduction of initial droplet velocity from 100 m/s (Fig.6b) to 0 (Fig.6a) tends to additional decrease of x_{evap} by 0.4 m. Reduction of W_1 flow from 90 m/s to 10 m/s leads to sharp decrease of x_{evap} (by 4-5 times), and increase of the initial temperature of air plasma flow from 2000 K to 4000 K (at $\beta=\beta^*$) does not influence $\boldsymbol{x}_{evap}$ significantly.

CONCLUSION

Based on the calculation results, the limiting values of the initial mass ratio of dispersed WONS and air-plasma flow ($\beta = \beta^*$) were determined, which ensure the final temperature of the flow $T_{end} \approx$ 1500 K in the reactor after complete evaporation of the droplets. At the initial temperatures of the air-plasma flow T_{g1} = 2000 K, 2600 K, 3000 K, 3600 K, and 4000 K β^* is 0.14, 0.26, 0.45, 0.76, and 1.20 respectively.

As a result of calculations carried out under these conditions using the developed mathematical model, regularities were established and a quantitative comparison of the effect of the initial values of the parameters of the air-plasma flow (temperature, velocity) and the WONS droplets (size, velocity) on the rate of their evaporation in the reactor was made. To achieve in the reactor the droplet complete evaporation zone $\boldsymbol{x}_{evap} \leq 1$ m, the following plasma processing modes of dispersed WONS in the air-plasma flow are necessary: $T_{g1} \geq$ 3600 K; $W_1 \leq$ 30 m/s; $a_{d1} \leq$ 40 μm; $V_1 \leq$ 10 m/s. The results of the research can be used to develop and optimize the operating modes of reactors designed for plasma processing of dispersed WONS in order to obtain fuel compositions for dispersion nuclear fuel.

ACKNOWLEDGMENT

The project was supported by the Russian Science Foundation (project 18-19-00136).

REFERENCES

1. D.M. Skorov, Yu. F. Bychkov and A.M. Dashkovskiy, *Reactor Material Science* (Atomizdat, Moscow, 1979) p.344.
2. A.G. Samoylov, A.I. Kashtanov and V.S. Volkov, *Dispersive Fuel Elements of Nuclear Reactors* (Atomizdat, Moscow, 1965) p.343.
3. S.V. Alekseev, V.A. Zaitsev and S.S. Tolstukhov, *Dispersion Nuclear Fuel* (Technosphere, Moscow, 2015), 248 p.
4. C. Degueldre and J.M. Paratte. J. Nucl. Mater. **274**, 1–6 (1999).
5. Yu. N. Tumanov, *Plasma and High Frequency Processes of Obtaining and Treatment of Materials in Nuclear Fuel Cycle: Present and Future* (Fizmatlit, Moscow, 2003) p.760.
6. R. Perekrestov, P. Kudrna, M. Tichy, I. Khalakhan and V. Myshkin. J. Phys. D: Appl. Phys. **49**, 265201 (2016).
7. P.V. Kosmachev, Y.A. Abzaev and V.A. Vlasov. Rus. Phys. J. **61**, 264–269 (2018).
8. D.G. Vidyaev, Yu.Yu. Lutsenko and E. Boretsky. IOP Conf. Ser.: Materials Science and Engineering. **135**, 1–5 (2016).
9. A.G. Karengin, A.A. Karengin, I.Y. Novoselov and N.V. Tundeshev. Adv. Mat. Res. **1040**, 433–436 (2014).
10. I.Yu. Novoselov, A.G. Karengin and R.G. Babaev. AIP Conf. Proc. **1938**, 1–5 (2018).
11. A.A. Kotelnikova, A.G. Karengin and O. Mendoza. AIP Conf. Proc. **1938**, 1–7 (2018).
12. I.V. Shamanin, A.G. Karengin, I.Yu. Novoselov, A.A. Karengin, E.S. Alyukov, A.D. Poberezhnikov, R.G. Babaev and O. Mendoza. J. Phys. Conf. Ser. **1145**, 1–7 (2019).
13. A.A. Karengin, A.G. Karengin and V.A. Vlasov. Rus. Phys. J. **58**, 730–736 (2015).
14. N.V. Vargaftik, *Reference Book of Thermophysical Properties of Gases and Liquids* (Nauka, Moscow, 1972), 720 p.
15. R. Rid and T. Sherwood, *Properties of Gases and Liquids* (Khimia, Leningrad, 1971), 704 p.